

REVIEW ARTICLE

Large-Scale Structure Observables in General Relativity

Donghui Jeong^{1,2} and Fabian Schmidt³

¹Department of Astronomy and Astrophysics, The Pennsylvania State University, University Park, PA 16802, USA

²Institute for Gravitation and the Cosmos, The Pennsylvania State University, University Park, PA 16802, USA

³Max-Planck-Institut für Astrophysik, Karl-Schwarzschild-Str. 1, D-85741 Garching, Germany

Abstract. We review recent studies that rigorously define several key observables of the large-scale structure of the Universe in a general relativistic context. Specifically, we consider i) redshift perturbation of cosmic clock events; ii) distortion of cosmic rulers, including weak lensing shear and magnification; iii) observed number density of tracers of the large-scale structure. We provide covariant and gauge-invariant expressions of these observables. Our expressions are given for a linearly perturbed flat Friedmann-Robertson-Walker metric including scalar, vector, and tensor metric perturbations. While we restrict ourselves to linear order in perturbation theory, the approach can be straightforwardly generalized to higher order.

PACS numbers: 98.65.Dx, 98.65.-r, 98.80.Jk

Submitted to: *Class. Quantum Grav.*

arXiv:1407.7979v2 [astro-ph.CO] 31 Jul 2014

1. Introduction

Over the past decade, cosmology has benefited from a vast increase in the available data [1, 2, 3, 4, 5, 6], which have been exploited through a variety of methods to probe the history and structure of the Universe. This trend will continue with future large surveys‡, and clearly, this calls for a rigorous investigation of what quantities precisely are observable from these surveys in the fully relativistic setting. Some observables have been investigated previously, most notably the number density of tracers [7, 8, 9, 10, 11, 12], the magnification, and to a lesser extent the shear [13, 14, 15].

In this review, we present a unified relativistic analysis of the observables from the large-scale structure of the Universe: *standard clocks*, *standard rulers*, and *number density of galaxies* (more generally, tracers). First, we consider a clock comoving with the cosmic fluid that shows the proper time elapsed since the Big Bang. The “apparent” age of the Universe at the same location is inferred using the observed redshift of the source. The difference between the two is an observable [16] that enters (often implicitly) in many different applications. For example, the cosmic microwave background on large scales (Sachs-Wolfe limit) can be thought of as one of the cosmic clock events.

A standard ruler [14] simply means that there is an underlying physical scale that we know of and we compare the observations to. This treatment applies to lensing measurements through galaxy ellipticities, sizes and fluxes, or through standard candles, to distortions of cosmological correlation functions, and to lensing of diffuse backgrounds. We show that in this framework, for ideal measurements, one can measure six degrees of freedom: a scalar on the sphere which corresponds to purely line-of-sight effects; a vector (on the sphere) which corresponds to mixed transverse/line-of-sight effects; and a symmetric transverse tensor on the sphere which comprises the shear and magnification [15]. We obtain general, gauge-invariant expressions for the six observable degrees of freedom, valid on the full sky. Throughout this paper, gauge invariance refers to the independence of the result on the choice of global perturbed FRW coordinates (say, e.g., comoving gauge vs conformal-Newtonian gauge). That is, the expressions are directly applicable to compare with observations and do not contain any unphysical coordinate artefacts.

The vector component and the shear admit a decomposition by parity into E/B -modes. The B -modes are free of all scalar contributions (including lensing as well as redshift-space distortions) at the linear level, making them ideal probes to look for tensor perturbations (gravitational waves). Throughout, we will work to linear order in perturbations, although the formalism can be straightforwardly extended to higher order.

Standard rulers in cosmology (again, think of mean size of a galaxy sample, or the correlation length of a tracer), are rarely absolute constants. Rather, they evolve in time, and this time evolution contributes at linear order to the observables described above through the variation in proper time since the Big Bang on a constant observed redshift surface. If one observes two spatially co-located rulers that evolve differently in time, one can isolate this effect. Thus, standard rulers can serve as cosmic clocks in the sense discussed above as well. The contribution of this effect to the magnification

‡ HETDEX (<http://www.hetdex.org>), eBOSS (<https://www.sdss3.org/future/eboss.php>), DESI (<http://desi.lbl.gov>), SuMIRe (<http://sumire.ipmu.jp/en/>), WFIRST-AFTA (<http://wfirst.gsfc.nasa.gov>), Euclid (<http://sci.esa.int/euclid/>), to list a few.

that we include in the calculation is *linear order* in metric perturbations but has previously been ignored.

Finally, we turn to another important large-scale structure observable, the number density of tracers such as galaxies [11, 12]. This requires two ingredients: the transformation of the volume element from apparent to physical volume, and the biasing relation between the density contrast of tracers and matter perturbations in the chosen gauge. The results for standard rulers and clocks can immediately be applied to derive these two contributions.

The outline of the paper is as follows: we begin in § 2 by spelling out the expression for null geodesics in a perturbed FRW spacetime, along with introducing our metric convention and useful notation. We then present the three large-scale observables in the subsequent sections: cosmic clock (§ 3), cosmic ruler (§ 4), and galaxy number density (§ 5). We conclude in § 6 with future perspective including the relevance of the effects to planned future surveys and further work needed to exploit the large-scale structure observables in general relativity. For all the quantitative results shown in this paper, we assume a flat Λ CDM cosmology with $h = 0.72$, $\Omega_m = 0.28$, a scalar spectral index $n_s = 0.958$ and power spectrum normalization at $z = 0$ of $\sigma_8 = 0.8$.

2. Light propagation in the perturbed universe

2.1. Notation

We use a conformal coordinate system (η, x^i) , and assume a spatially flat FRW background metric $\bar{g}_{\mu\nu} = a^2(\eta)\eta_{\mu\nu}$. The linearly perturbed FRW metric is written as

$$ds^2 = a^2(\eta) \left[-(1 + 2A)d\eta^2 - 2B_i d\eta dx^i + (\delta_{ij} + h_{ij}) dx^i dx^j \right]. \quad (1)$$

We will work to linear order in A, B, h throughout. Latin indices i, j, k, \dots denote spatial coordinates, and Greek indices $\mu, \nu, \rho, \sigma, \dots$ denote the space-time coordinates. Unless otherwise indicated, we raise and lower space-time indices with the full metric Equation (1), and space indices by δ_{ij} . For scalar perturbations, the spatial part is often further expanded as $h_{ij} = 2(D\delta_{ij} + E_{ij})$, where E_{ij} is symmetric and traceless. We denote the trace of h_{ij} as $h \equiv \delta^{ij} h_{ij}$. In § 4, we shall also present results in two popular gauges: the synchronous-comoving (sc) gauge, where $A = 0 = B_i$, so that

$$ds^2 = a^2(\eta) \left[-d\eta^2 + (\delta_{ij} + h_{ij}) dx^i dx^j \right]; \quad (2)$$

and the conformal-Newtonian (cN) gauge, where $B_i = 0 = E_{ij}$, so that (with $A = \Psi$, $D = \Phi$)

$$ds^2 = a^2(\eta) \left[-(1 + 2\Psi)d\eta^2 + (1 + 2\Phi)\delta_{ij} dx^i dx^j \right]. \quad (3)$$

It is useful to define projection operators parallel (\parallel) and perpendicular (\perp) to the observed line-of-sight direction \hat{n}^i , so that for any spatial vector X^i and tensor h_{ij} ,

$$\begin{aligned} X_{\parallel} &\equiv \hat{n}_i X^i, \quad h_{\parallel} \equiv \hat{n}_i \hat{n}_j h^{ij}, \\ X_{\perp}^i &\equiv \mathcal{P}^{ij} X_j, \quad \mathcal{P}^{ij} \equiv \delta^{ij} - \hat{n}^i \hat{n}^j. \end{aligned} \quad (4)$$

Correspondingly, we define projected derivative operators,

$$\partial_{\parallel} \equiv \hat{n}^i \partial_i, \quad \text{and} \quad \partial_{\perp}^i \equiv \mathcal{P}^{ij} \partial_j. \quad (5)$$

Note that ∂_{\perp}^i , ∂_{\parallel} and ∂_{\perp}^i , ∂_{\perp}^j do not commute, while \hat{n}^i and ∂_{\parallel} do commute. Further, we find

$$\partial_j \hat{n}^i = \partial_{\perp j} \hat{n}^i = \frac{1}{\chi} \mathcal{P}_j^i, \quad (6)$$

where χ is the norm of the position vector so that $\hat{n}^i = x^i/\chi$. More expressions can be found in § II of [11].

We further decompose quantities defined on the sphere, i.e. functions of the unit line-of-sight vector $\hat{\mathbf{n}}$, in terms of their properties under a rotation around $\hat{\mathbf{n}}$. Let $(\mathbf{e}_1, \mathbf{e}_2, \hat{\mathbf{n}})$ denote an orthonormal coordinate system. If we rotate the coordinate system around $\hat{\mathbf{n}}$ by an angle ψ , so that $\mathbf{e}_i \rightarrow \mathbf{e}'_i$, then the linear combinations $\mathbf{m}_{\pm} \equiv (\mathbf{e}_1 \mp i \mathbf{e}_2)/\sqrt{2}$ transform as

$$\mathbf{m}_{\pm} \rightarrow \mathbf{m}'_{\pm} = e^{\pm i\psi} \mathbf{m}_{\pm}. \quad (7)$$

A general function, or, more properly, tensor component $f(\hat{\mathbf{n}})$ is called spin- s if it transforms under the same transformation as

$$f(\hat{\mathbf{n}}) \rightarrow f(\hat{\mathbf{n}})' = e^{is\psi} f(\hat{\mathbf{n}}). \quad (8)$$

An ordinary scalar function on the sphere is clearly spin 0, while the unit vectors \mathbf{m}_{\pm} defined above are spin ± 1 fields. This decomposition is particularly useful for deriving multipole coefficients and angular power spectra. We also define

$$X_{\pm} \equiv m_{\mp}^i X_i, \quad h_{\pm} \equiv m_{\mp}^i m_{\mp}^j h_{ij} \quad (9)$$

for any 3-vector X_i and 3-tensor h_{ij} .

2.2. Integration of geodesic equation

Cosmological observations are made by collecting light from distant sources (e.g. galaxies) and measuring their positions, fluxes, shapes, and redshifts. The relativistic effects we discuss in this paper are due to the displacement between the intrinsic spacetime location of sources and their apparent location inferred from the observed angular coordinate $\hat{\mathbf{n}}$ and redshift z by using the background FRW metric (see Fig. 1). In this section, we outline the derivation of the displacements for a source comoving with the cosmic fluid[§] (see also [17]) described by the four velocity

$$u^{\mu} = a^{-1} (1 - A, v^i), \quad u_{\mu} = a (-1 - A, v_i - B_i) \quad (10)$$

in the general gauge given by Equation (1). Note that we take care to include all the contributions explicitly, including those which only contribute to the monopole. These contributions are essential when verifying the expressions through test cases as described in the appendices of [11, 14, 16].

Choosing the background comoving distance χ as affine parameter, the conformal photon momentum may be written as

$$\frac{dx^{\mu}}{d\chi} = (-1 + \delta\nu(\chi), \hat{n}^i + \delta e^i(\chi)), \quad (11)$$

with the fractional frequency shift $\delta\nu$ and the deflection δe^i of the photon along the geodesic. The light propagation in the perturbed FRW metric is described by the geodesic equation

$$\frac{d}{d\chi} \frac{dx^{\mu}}{d\chi} + \Gamma_{\alpha\beta}^{\mu} \frac{dx^{\alpha}}{d\chi} \frac{dx^{\beta}}{d\chi} = 0. \quad (12)$$

[§] The assumptions of comoving source and observer are easily relaxed to allow for general motion.

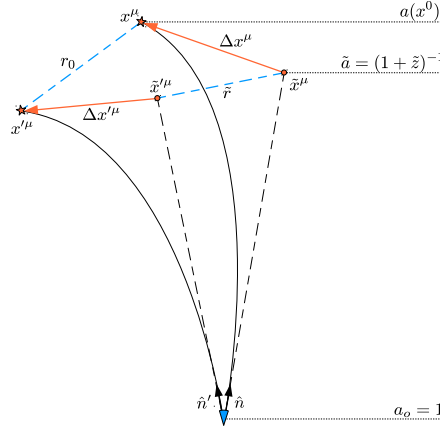


Figure 1. Sketch of perturbed photon geodesics illustrating our notation (from [14]). The observer is located at the bottom. Photons arrive out of the observed directions $\hat{\mathbf{n}}, \hat{\mathbf{n}}'$ and with observed redshifts \tilde{z}, \tilde{z}' . The solid lines indicate the actual photon geodesics tracing back to the sources indicated by stars. The dashed lines show the apparent background photon geodesics tracing back to the inferred source positions indicated by circles, perturbed from the actual positions by the displacements $\Delta x^\mu, \Delta x'^\mu$ (whose magnitude is greatly exaggerated here). \tilde{r} is the apparent spatial separation between the endpoints (apparent size of the ruler), while r_0 is the true separation.

The zeroth order geodesic equation is just $dx^\mu/d\chi = \text{constant}$, which yields the background geodesic,

$$\bar{x}^\mu(\chi) = (\eta_0 - \chi, \hat{\mathbf{n}}\chi), \quad (13)$$

where η_0 is the conformal time at present where the observation is made. Equation (13) determines the apparent position \tilde{x}^μ of a source with observed redshift \tilde{z} and angular position \hat{n}^i as $\tilde{x}^\mu = (\eta_0 - \tilde{\chi}, \hat{n}^i \tilde{\chi})$ with $\tilde{\chi} \equiv \bar{\chi}(\tilde{z})$ being the comoving distance-redshift relation in the background Universe. Hereafter, we shall use tilde to refer to the observed (or apparent) quantities, and bar to refer to background quantities.

At linear order, the temporal and spatial components of the geodesic equation read

$$\frac{d}{d\chi} (\delta\nu - 2A) = \dot{A} - \frac{1}{2}\dot{h}_\parallel - \partial_\parallel B_\parallel \quad (14)$$

$$\frac{d}{d\chi} (\delta e^i + B^i + h^i_j \hat{n}^j) = -\partial_i A + \partial_i B_\parallel - B_{\perp i} + \frac{1}{2}\partial_i h_\parallel - \frac{1}{\chi} \mathcal{P}^{ij} h_{jk} \hat{n}^k. \quad (15)$$

Here and throughout, a dot represents the derivative with respect to conformal time. We integrate the geodesic equation starting from the comoving observer at $\chi = 0$. We choose him or her to lie at the spatial origin $\mathbf{0}$, and to observe at a fixed *proper time* t_o [see Eq. (33) in the next section]:

$$t_o = \int_0^{\eta_o} [1 + A(\mathbf{0}, \eta')] a(\eta') d\eta'. \quad (16)$$

Note that this is a coordinate independent way of defining the observation time, and we normalize the scale factor with the proper time at observation through $a(t_o) = 1$

following the usual convention. Then, the scale factor in the metric Equation (1) at observation differs from the background value by $\delta a_o = a_o - 1$:

$$\delta a_o = -\left.\frac{da}{dt}\right|_o \int_0^{t_o} A(\mathbf{0}, \bar{\eta}(t)) dt = -H_0 \int_0^{t_o} A(\mathbf{0}, \bar{\eta}(t)) dt. \quad (17)$$

In what follows, the subscript $_o$ will refer to quantities evaluated at the observer's spacetime location.

The initial conditions of $\delta\nu$, δe^i at the observation are fixed by the requirement that the observed (past-directed) photon four momentum is $(1, \hat{n}^i)$. An orthonormal tetrad $(e_a)^\mu$ for an observer comoving with the cosmic fluid (as we will assume throughout) is given by

$$\begin{aligned} (e_0)^\mu &= a^{-1} (1 - A, v^i) \\ (e_j)^\mu &= a^{-1} \left(v_j - B_j, \delta_j^i - \frac{1}{2} h_j^i \right). \end{aligned} \quad (18)$$

Here, we use $a, b = 0, 1, 2, 3$ for the space-time index of the tetrad (e_a) , while $\mu, \nu = 0, 1, 2, 3$ denotes the coordinate index of the tetrad $(e_a)^\mu$. Then, the observed energy and momentum at $\chi = 0$ are, respectively,

$$1 = [a^{-2} g_{\mu\nu} (e_0)^\mu p^\nu]_o, \quad \hat{n}_i = [a^{-2} g_{\mu\nu} (e_i)^\mu p^\nu]_o, \quad (19)$$

from which we find the initial conditions as

$$\begin{aligned} \delta\nu_0 &= -\delta a_o + A_o + v_{\parallel o} - B_{\parallel o} \\ \delta e_o^i &= \delta a_o \hat{n}^i - v_o^i - \frac{1}{2} (h^i_j)_o \hat{n}^j. \end{aligned} \quad (20)$$

The a^{-2} factors in Eq. (19) come from the transformation of the affine parameter with respect to the conformal metric (χ) to that corresponding to the physical metric (λ) through $d\chi/d\lambda = a^{-2}$ [11].

Given the initial conditions Equation (20), we now integrate the geodesic equation twice to yield the temporal and spatial displacements:

$$\begin{aligned} \delta x^0(\chi) &= [-\delta a_o - A_o + v_{\parallel o} - B_{\parallel o}] \chi \\ &+ \int_0^\chi d\chi' \left[2A + (\chi - \chi') \left\{ \dot{A} - \frac{1}{2} \dot{h}_{\parallel} - \partial_{\parallel} B_{\parallel} \right\} \right] - \int_0^{t_o} A(\mathbf{0}, t) dt \end{aligned} \quad (21)$$

$$\begin{aligned} \delta x^i(\chi) &= \left[\delta a_o \hat{n}^i + \frac{1}{2} (h^i_j)_o \hat{n}^j + B_o^i - v_o^i \right] \chi \\ &+ \int_0^\chi d\chi' \left[-B^i - h^i_j \hat{n}^j + (\chi - \chi') \left\{ -\partial_i A + \hat{n}^j \partial_i B_j + \frac{1}{2} (\partial_i h_{jk}) \hat{n}^j \hat{n}^k \right\} \right]. \end{aligned} \quad (22)$$

Here, we used $\delta x^i(\chi = 0) = 0$ as spatial boundary condition at the observer. The temporal boundary condition employed in Eq. (21) is determined through the fixed proper time of observation, Equation (16), and $\delta x^0(\chi = 0) = \eta_o - \bar{\eta}(t_o)$ where $\bar{\eta}(\bar{t})$ is the background conformal time–physical time relation.

The final ingredient that we need to complete the calculation is the affine parameter at emission of the photon, $\chi_e = \tilde{\chi} + \delta\chi$. This is fixed by requiring the photon frequency to match the observed redshift \tilde{z} . From the tetrad in Equation (18), \tilde{z} is given by the ratio between the photon energy at emission and observation as:

$$1 + \tilde{z} \equiv \frac{1}{\tilde{a}} = \frac{[a^{-2} g_{\mu\nu} (e_o)^\mu p^\nu]_e}{[a^{-2} g_{\mu\nu} (e_o)^\mu p^\nu]_o} = \frac{1}{a(x^0)} (1 + A - \delta\nu + v_{\parallel} - B_{\parallel}). \quad (23)$$

Here, all quantities on the right hand side are evaluated at emission. We find it convenient to define the perturbation to the logarithm of the scale factor at emission $\Delta \ln a \equiv a(x^0)/\tilde{a} - 1$. Equation (23) yields

$$\Delta \ln a = A_o - A + v_{\parallel} - v_{\parallel o} + \int_0^{\tilde{\chi}} d\chi \left[-\dot{A} + \frac{1}{2}\dot{h}_{\parallel} + \dot{B}_{\parallel} \right] - H_0 \int_0^{t_o} A(\mathbf{0}, \bar{\eta}(t)) dt. \quad (24)$$

The redshift matching then requires

$$\Delta \ln a = \left. \frac{\partial \ln a}{\partial \eta} \right|_{\tilde{z}} (x^0 - \tilde{x}^0) = \frac{H(\tilde{z})}{1 + \tilde{z}} (\delta x^0(\tilde{\chi}) - \delta \chi). \quad (25)$$

We can then solve for the perturbation to the affine parameter yielding

$$\delta \chi = \delta x^0(\tilde{\chi}) - \frac{1 + \tilde{z}}{H(\tilde{z})} \Delta \ln a. \quad (26)$$

The actual source position is at linear order

$$x^\mu(\chi_e) = \bar{x}^\mu(\chi_e) + \delta x^\mu(\tilde{\chi}) = \bar{x}^\mu(\tilde{\chi}) + [\bar{x}^\mu(\chi_e) - \bar{x}^\mu(\tilde{\chi})] + \delta x^\mu(\tilde{\chi}). \quad (27)$$

To linear order, this gives

$$\begin{aligned} \Delta x^0 &\equiv x^0 - \tilde{x}^0 = \delta x^0(\tilde{\chi}) - \delta \chi \\ \Delta x^i &\equiv x^i - \tilde{x}^i = \delta x^i(\tilde{\chi}) + \hat{n}^i \delta \chi. \end{aligned} \quad (28)$$

Finally, we assemble the deflection along the line of sight direction as

$$\begin{aligned} \Delta x_{\parallel} &= \hat{n}_i \Delta x^i = \delta x_{\parallel} + \delta x^0 - \frac{1 + \tilde{z}}{H(\tilde{z})} \Delta \ln a \\ &= - \int_0^{t_o} A(\mathbf{0}, t) dt + \int_0^{\tilde{\chi}} d\chi \left[A - B_{\parallel} - \frac{1}{2} h_{\parallel} \right] - \frac{1 + \tilde{z}}{H(\tilde{z})} \Delta \ln a. \end{aligned} \quad (29)$$

The transverse displacement $\Delta x_{\perp}^i = \mathcal{P}^i_j \Delta x^j$ is given by

$$\begin{aligned} \Delta x_{\perp}^i &= \left[\frac{1}{2} \mathcal{P}^{ij} (h_{jk})_o \hat{n}^k + B_{\perp o}^i - v_{\perp o}^i \right] \tilde{\chi} - \int_0^{\tilde{\chi}} d\chi \left[\frac{\tilde{\chi}}{\chi} (B_{\perp}^i + \mathcal{P}^{ij} h_{jk} \hat{n}^k) \right. \\ &\quad \left. + (\tilde{\chi} - \chi) \partial_{\perp}^i \left(A - B_{\parallel} - \frac{1}{2} h_{\parallel} \right) \right]. \end{aligned} \quad (30)$$

3. Cosmic clock

Perhaps the simplest general relativistic observables are cosmic clocks [16], or standard clocks, a set of events whose proper time (local age of the universe) is accurately known. These cosmic clock events define an observable $\mathcal{T}(\hat{n})$ as the difference in logarithm of scale factor ($\ln a$) between a constant-proper-time hypersurface $t_F = \text{const}$ and a constant-observed-redshift surface $\tilde{z} = \text{const}$. Although phrased as a perturbation in $\ln a$, we will frequently refer to \mathcal{T} loosely as the proper time perturbation. This is because at leading order, the perturbation to the proper time $\Delta t_F(\hat{\mathbf{n}})$ at observed redshift \tilde{z} is simply related to \mathcal{T} through

$$\Delta t_F(\hat{\mathbf{n}}) = H^{-1}(\tilde{z}) \mathcal{T}(\hat{\mathbf{n}}). \quad (31)$$

Since \mathcal{T} is defined through two observationally well-defined quantities (proper time and observed redshift), it is an observable, and the expression for \mathcal{T} is gauge-invariant.

The proper time interval dt_F along the geodesic of a comoving observer is at linear order given by

$$dt_F = \sqrt{-g_{\mu\nu}dx^\mu dx^\nu} = (1 + A)ad\eta. \quad (32)$$

Integrating Equation (32), we obtain an expression for $t_F|_x$, the proper time of a comoving source passing through \mathbf{x} at coordinate time x^0 , at linear order

$$t_F|_x = \int_0^{x^0} [1 + A(\mathbf{x}, \eta')] a(\eta') d\eta'. \quad (33)$$

In the case at hand, x^0 is the coordinate time at emission, which is different from the coordinate time $\bar{\eta}(t_F|_x)$ in an unperturbed universe at the proper time t_F . The ratio of scale factors at coordinate time x^0 and $\bar{\eta}(t_F|_x)$ is

$$\frac{a[\bar{\eta}(t_F|_x)]}{a(x^0)} = 1 + H(x^0) \int_0^{x^0} A(\mathbf{x}, \eta') a(\eta') d\eta'. \quad (34)$$

The observable $\mathcal{T}(\tilde{x})$ is defined through

$$\mathcal{T}(\tilde{x}) \equiv \ln \left(\frac{a[\bar{\eta}(t_F|\tilde{x})]}{\tilde{a}} \right), \quad (35)$$

where $\tilde{a} = (1 + \tilde{z})^{-1}$ is the apparent scale factor at emission. Since $\ln[a(x^0)/\tilde{a}]$ is precisely the perturbation $\Delta \ln a$ derived in § 2, we arrive at the following simple expression for \mathcal{T} :

$$\mathcal{T} = \ln \left(\frac{a(x^0)}{\tilde{a}} \frac{a[\bar{\eta}(t_F|\tilde{x})]}{a(x^0)} \right) = \Delta \ln a + \tilde{H} \int_0^{\bar{\eta}} A[\mathbf{x}, \eta'] a(\eta') d\eta', \quad (36)$$

where $\tilde{H} \equiv H(\tilde{z})$. The gauge invariance of the observable \mathcal{T} is explicitly shown in the Appendix A of [16]. The numerical result for the power spectrum of \mathcal{T} induced by a standard power spectrum of scale-invariant curvature perturbations in Λ CDM is shown in Fig. 3.

A cosmic clock exists whenever we have an observable from which we can define a constant proper-time hypersurface. There are two such classes of observables: 1) cosmic events defined by a unique time and sufficiently short duration, 2) observables with known time evolution. Cosmic recombination, which led to the emission of the cosmic microwave background (CMB) is an example of the former. Neglecting all perturbations including sound waves, last scattering of the Cosmic Microwave Background (CMB) photons happened at a fixed proper time in the local frame, and, therefore, is a cosmic clock event. On scales larger than the angular size of the sound horizon at recombination, the temperature perturbations in the CMB are then exactly given by $\Theta(\hat{n}) = -\mathcal{T}(\hat{n})$ (Sachs-Wolfe limit [18, 16]). The exact same equation applies in describing the perturbations in, for example, the surface of neutrino decoupling, Big-Bang Nucleosynthesis and thermal decoupling of baryons from CMB on super-horizon scales. The second case is exemplified by time varying cosmic rulers, which will be discussed in the next section.

4. Cosmic ruler, or generalized weak gravitational lensing

We now move on to the cosmic ruler, with which we mean a known spatial scale in the comoving frame of the cosmic fluid. This could be the size of a galaxy, or the length at which the correlation function reaches a certain value (we will discuss these

applications in § 4.6). What we observe is the *apparent* size of this “ruler”, inferred using the observed positions and redshifts of the endpoints. By comparing this to the known spatial scale, we can infer the departure from the average angular diameter distance-redshift relation and the Hubble parameter-redshift relation. In many cases, the size of the ruler will only be known in a statistical sense (for example, galaxy sizes) and will be calibrated by averaging over the entire area of a given survey. Any scatter in the ruler size from its mean value will simply be noise in the measurement of the ruler distortions, as long as this scatter is not correlated with large-scale perturbations themselves. The latter, “intrinsic” contributions to the distortion of the ruler scale will not be considered in this paper, although they can be an important source of cosmological information on their own [19, 20, 21, 22, 23, 24, 15, 25].

As we shall show below, the ruler distortions can be decomposed into scalar, vector, and tensor components on the observer’s sky. The tranverse “sky-plane” components, one scalar and two tensor components, are nothing other than the standard lensing observables of magnification and shear, respectively. The remaining distortions, one scalar and two vector components on the sky, involve the line-of-sight component of the ruler. Typically, these can only be observed through spectroscopic measurements, since the line-of-sight separation, inferred from the redshift difference between the two endpoints, has to be measured with sufficient accuracy. When applied to correlation functions, these distortions are part of the well-known redshift-space distortion effects. However, we stress that the expressions we derive are entirely independent of the nature of the ruler considered, and that spectroscopic LSS surveys are just one (albeit important) application of these new observables.

A standard ruler can be generically modeled by two spacetime events separated by a fixed spacelike separation r_0 on a fixed proper time surface of the cosmic fluid. More precisely, the spatial part of the four-velocity u^μ of this fluid is determined by

$$v^i = \frac{T^i_0}{\rho + p}. \quad (37)$$

This ruler definition can also be phrased as that the length of the ruler is defined on a surface of constant proper time of comoving observers. This proper time corresponds to the “local age” of the Universe. We are mostly interested in applications to the large-scale structure during matter domination. In this case, the cosmic fluid is simply matter (dark matter + baryons), and there is no ambiguity in this definition; in synchronous-comoving gauge, Equation (37) yields $v^i = 0$. However, this assumption can be relaxed very easily, for example one could assume instead that the observers are comoving with the baryon velocity v_b .

Then, what we observe is the apparent size of the ruler. Let $\hat{\mathbf{n}}, \tilde{z}$ and $\hat{\mathbf{n}}', \tilde{z}'$ denote the observed coordinates of the endpoints of the ruler, and $\tilde{\mathbf{x}}$ and $\tilde{\mathbf{x}}'$ the apparent spatial positions inferred through Equation (13) (see Fig. 1). In the following, we will assume that the ruler is small compared to the distance $\tilde{\chi}$ of the sources as well as to the typical scale over which we want to measure the spacetime perturbations; it can then be approximated as an infinitesimal distance. For example, in terms of weak lensing observables, we assume that the angular size of a galaxy is negligible compared to the angular scale at which we measure shear correlations. Corrections to this approximation involve powers of $|\tilde{\mathbf{x}} - \tilde{\mathbf{x}}'|/\tilde{\chi}$ (wide-angle corrections), and/or higher derivatives of the metric perturbations multiplied by powers of $x^\mu - x'^\mu$.^{||} The

^{||} For example, for the sky-plane components the leading order correction of this type corresponds to the lensing flexion. If desired one could straightforwardly extend the treatment to obtain a covariant

apparent physical length of the cosmic ruler is then given by

$$\tilde{r}^2 = \tilde{a}^2 \delta_{ij} (\tilde{x}^i - \tilde{x}'^i) (\tilde{x}^j - \tilde{x}'^j), \quad (38)$$

where $\tilde{a} = 1/(1 + \tilde{z})$ is the observationally inferred scale factor at emission (Fig. 1). The actual separation of the two endpoints of the ruler, x^μ , x'^μ , as measured in the comoving frame, on the other hand should be equal to the fixed scale r_0 :

$$[g_{\mu\nu}(x^\alpha) + u_\mu(x^\alpha)u_\nu(x^\alpha)](x^\mu - x'^\mu)(x^\nu - x'^\nu) = r_0^2. \quad (39)$$

The four-velocity of comoving observers, whose spatial components are fixed by Equation (37), is given by Eq. (10). With this, Equation (39) yields

$$\begin{aligned} & -2\tilde{a}^2 v_i \{ \delta\tilde{x}^0 \delta\tilde{x}^i + \delta\tilde{x}^0 [\Delta x^i - \Delta x'^i] + \delta\tilde{x}^i [\Delta x^0 - \Delta x'^0] \} \\ & + g_{ij}(x^\alpha) \left\{ \delta\tilde{x}^i \delta\tilde{x}^j + \delta\tilde{x}^i [\Delta x^j - \Delta x'^j] + [\Delta x^i - \Delta x'^i] \delta\tilde{x}^j \right\} = r_0^2, \end{aligned} \quad (40)$$

where $\Delta x^\mu = \Delta x^\mu(\hat{\mathbf{n}}, \tilde{z})$, $\Delta x'^\mu = \Delta x^\mu(\hat{\mathbf{n}}', \tilde{z}')$, and the components of the *apparent* separation vector are $\delta\tilde{x}^\mu = \tilde{x}^\mu - \tilde{x}'^\mu$. In order to evaluate the spatial metric $g_{ij}(x^\alpha)$ at the location of the ruler, we use $\Delta \ln a = a(x^0)/\tilde{a} - 1$ to obtain at first order

$$g_{ij}(x^\alpha) = \tilde{a}^2 [(1 + 2\Delta \ln a) \delta_{ij} + h_{ij}]. \quad (41)$$

We now again make use of the ‘‘small ruler’’ approximation, so that

$$\Delta x^i - \Delta x'^i \simeq \delta\tilde{x}^\alpha \frac{\partial}{\partial \tilde{x}^\alpha} \Delta x^i. \quad (42)$$

Like any vector, we can decompose the spatial part of the apparent separation $\delta\tilde{x}^i$ into parts parallel and transverse to the line of sight:

$$\begin{aligned} \delta\tilde{x}_\parallel &\equiv \hat{n}_i \delta\tilde{x}^i \\ \delta\tilde{x}_\perp^i &\equiv \mathcal{P}^i_j \delta\tilde{x}^j = \delta\tilde{x}^i - \hat{n}^i \delta\tilde{x}_\parallel. \end{aligned} \quad (43)$$

In the correlation function literature, $\delta\tilde{x}_\parallel$, $|\delta\tilde{\mathbf{x}}_\perp|$ are often referred to as π and σ , respectively. Then,

$$\delta\tilde{x}^\alpha \frac{\partial}{\partial \tilde{x}^\alpha} = (\delta\tilde{x}^0 \partial_\eta + \delta\tilde{x}_\parallel \partial_\parallel) + \delta\tilde{x}_\perp^i \partial_{\perp i}, \quad (44)$$

where we have similarly defined $\partial_\parallel = \hat{n}^i \partial_i$, $\partial_{\perp i} = \mathcal{P}_i^j \partial_j$. Since the observed coordinates \tilde{x}^μ by definition satisfy the light cone condition with respect to the unperturbed FRW metric, we have $\delta\tilde{x}^0 = -\delta\tilde{x}_\parallel$ in the small-angle approximation. Thus,

$$\delta\tilde{x}^0 \partial_\eta + \delta\tilde{x}_\parallel \partial_\parallel = \delta\tilde{x}_\parallel (\partial_\parallel - \partial_\eta) = \delta\tilde{x}_\parallel \frac{\partial}{\partial \tilde{\chi}} = \delta\tilde{x}_\parallel H(\tilde{z}) \frac{\partial}{\partial \tilde{z}}, \quad (45)$$

where $\partial/\partial \tilde{\chi}$ is the derivative with respect to the affine parameter at emission. We thus have

$$\delta\tilde{x}^\alpha \frac{\partial}{\partial \tilde{x}^\alpha} = \delta\tilde{x}_\parallel \partial_{\tilde{\chi}} + \delta\tilde{x}_\perp^i \partial_{\perp i}. \quad (46)$$

Working to first order in perturbations, we then obtain

$$\begin{aligned} r_0^2 - \tilde{r}^2 &= 2\Delta \ln a \tilde{r}^2 + \tilde{a}^2 h_{ij} \delta\tilde{x}^i \delta\tilde{x}^j + 2\tilde{a}^2 \left(v_\parallel \delta\tilde{x}_\parallel^2 + v_{\perp i} \delta\tilde{x}_\perp^i \delta\tilde{x}_\perp^i \right) \\ &\quad + 2\tilde{a}^2 \delta_{ij} \delta\tilde{x}^i (\delta\tilde{x}_\parallel \partial_{\tilde{\chi}} + \delta\tilde{x}_\perp^k \partial_{\perp k}) \Delta x^j. \end{aligned} \quad (47)$$

All terms are straightforward to interpret: there are the perturbations to the metric at the ruler location (both from the metric perturbation h_{ij} and the perturbation to the scale factor at emission); the contribution $\propto v$ from the projection from fixed- η to fixed-proper-time hypersurfaces; and the difference in the spatial displacements of the endpoints of the ruler.

expression for the flexion.

4.1. Clocks and evolving rulers

In the previous section, we have implicitly assumed, as is usually done, that the ruler scale is constant in time, i.e. a non-evolving ruler. However, in many instances in cosmology, rulers do evolve over time; that is, the ruler scale r_0 depends on the local age of the Universe (proper time of the comoving observer). For example, the mean size of galaxies evolves, and so does the correlation length of large-scale structure tracers. Thus, cosmic rulers in general are also cosmic clocks (§ 3).

Let us consider a standard ruler whose length evolves in time. Then, by using Equation (34), we can parametrize the time evolution of the proper size of the standard ruler $r_0(a)$ through its value in an unperturbed Universe as function of the scale factor a . The actual proper size of the ruler $r_0(a(t_F|x))$, which is the size of the ruler in the constant-proper-time slicing, relative to the size it evaluates to when inserting the apparent scale factor of emission $\tilde{a} = (1 + \tilde{z})^{-1}$, in the constant-observed-redshift slicing, is given by

$$\frac{r_0(a(t_F|x))}{r_0(\tilde{a})} = 1 + \frac{d \ln r_0(\tilde{a})}{d \ln \tilde{a}} \mathcal{T}(\tilde{x}), \quad (48)$$

where \mathcal{T} is defined in Eq. (36). Note that we are assuming that $a_o = 1$ at observation, Equation (17), so that $r_0(1)$ corresponds to the ruler scale today as calibrated by the observer. This clearly requires that $\mathcal{T} = 0$ for a locally measured ruler, which is the case for Eq. (36). To reach this consistency, it is essential that the epoch of observation t_o is fixed in terms of proper time, rather than coordinate time, as discussed in § 2.

We thus have an additional contribution to the ruler distortion Equation (47) which is proportional to the time derivative of the ruler, explicitly

$$- 2\mathcal{T} \frac{d \ln r_0(\tilde{a})}{d \ln \tilde{a}} \tilde{r}^2. \quad (49)$$

4.2. Scalar-vector-tensor decomposition on the sky

It is useful to separate the contributions to Equation (47) in terms of the observed longitudinal and transverse distortions. For some applications, only the transverse distortions are relevant. This is the case for diffuse backgrounds without redshift resolution, such as the CMB or the cosmic infrared background, and largely the case for photometric galaxy surveys. On the other hand, spectroscopic surveys and redshift-resolved backgrounds such as the 21cm emission from high-redshifts are able to measure the longitudinal displacements as well.

Noting that $\tilde{r}^2 = \tilde{a}^2[\delta\tilde{x}_\parallel^2 + (\delta\tilde{\mathbf{x}}_\perp)^2]$, and taking the square root of Equation (47), we obtain the relative perturbation to the physical scale of the ruler as

$$\frac{\tilde{r} - r_0}{\tilde{r}} = \mathcal{C} \frac{(\delta\tilde{x}_\parallel)^2}{\tilde{r}_c^2} + \mathcal{B}_i \frac{\delta\tilde{x}_\parallel \delta\tilde{x}_\perp^i}{\tilde{r}_c^2} + \mathcal{A}_{ij} \frac{\delta\tilde{x}_\perp^i \delta\tilde{x}_\perp^j}{\tilde{r}_c^2}, \quad (50)$$

where we have defined $\tilde{r}_c \equiv \tilde{r}/\tilde{a}$ as the apparent comoving size of the ruler. The quantities multiplying \mathcal{C} , \mathcal{B}_i , \mathcal{A}_{ij} are thus simply geometric factors. The coefficients are given by

$$\begin{aligned} \mathcal{C} &= \frac{d \ln r_0(\tilde{a})}{d \ln \tilde{a}} \mathcal{T} - \Delta \ln a - \frac{1}{2} h_\parallel - v_\parallel - \partial_{\tilde{x}} \Delta x_\parallel \\ \mathcal{B}_i &= -\mathcal{P}_i^j h_{jk} \hat{n}^k - v_{\perp i} - \hat{n}^k \partial_{\perp i} \Delta x_k - \partial_{\tilde{x}} \Delta x_{\perp i} \\ \mathcal{A}_{ij} &= \frac{d \ln r_0(\tilde{a})}{d \ln \tilde{a}} \mathcal{T} \mathcal{P}_{ij} - \Delta \ln a \mathcal{P}_{ij} - \frac{1}{2} \mathcal{P}_i^k \mathcal{P}_j^l h_{kl} \end{aligned}$$

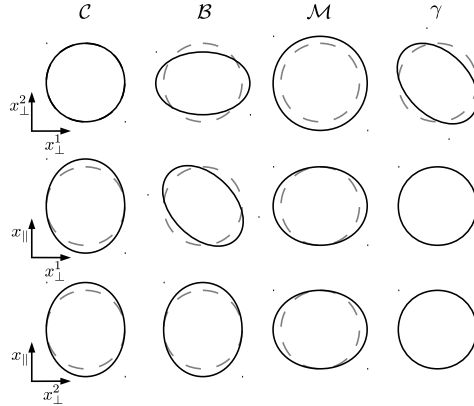


Figure 2. Illustration of the distortion of standard rulers due to the longitudinal (2-)scalar \mathcal{C} , (2-)vector \mathcal{B} , and transverse components, magnification \mathcal{M} and shear γ . The first row shows the projection onto the sky plane, while the second (third) row show the projection onto the line-of-sight and x_{\perp}^1 (x_{\perp}^2) axes, respectively. In case of \mathcal{B} and γ , we only show one of the two components. From [14]; see also Fig. 3 in [26].

$$-\frac{1}{2}(\mathcal{P}_{jk}\partial_{\perp i} + \mathcal{P}_{ik}\partial_{\perp j})\Delta x^k, \quad (51)$$

where Δx_{\parallel} , Δx_{\perp}^i are the parallel and perpendicular components of the displacements Δx^i . Note that while we have assumed that the ruler is small, the expressions for \mathcal{C} , \mathcal{B}_i , \mathcal{A}_{ij} are valid on the full sky. Fig. 2 illustrates the distortions induced by these components. Observationally, we have 6 free parameters (assuming accurate redshifts are available): the location of one point $\hat{\mathbf{n}}$, \tilde{z} , and the separation vector described by $\delta\tilde{x}^i$ (with $\delta\tilde{x}^0$ being fixed by the light cone condition). Using these, we can measure a (2-)scalar on the sphere, \mathcal{C} , a 2×2 symmetric matrix, \mathcal{A}_{ij} , and a 2-component vector on the sphere, \mathcal{B}_i . As a symmetric matrix on the sphere, \mathcal{A}_{ij} has a scalar component, given by the trace $\mathcal{M} \equiv \mathcal{P}^{ij}\mathcal{A}_{ij}$ (*magnification*), and two components of the traceless part which transform as spin-2 fields on the sphere (*shear*, $\pm 2\gamma$ as defined in Equation (69) below). These quantities are observable and gauge-invariant, although any of the individual contributions in Equation (51) are not. The only exception is the proper time perturbation \mathcal{T} , which can be isolated by comparing two co-located rulers which evolve differently in time. Note that we cannot measure any of the anti-symmetric components, such as the rotation. This is because we have not assumed the existence of any preferred directions in the Universe. If there is a primary spin-1 or higher spin field, such as the polarization in case of the CMB, then a rotation can be measured as it mixes the spin ± 2 components (see, e.g. [27]). In the next sections we study the three terms \mathcal{C} , \mathcal{B}_i , \mathcal{A}_{ij} in turn.

4.3. Longitudinal scalar

The longitudinal component can be simplified to become

$$\mathcal{C} = \frac{d \ln r_0(\tilde{a})}{d \ln \tilde{a}} \mathcal{T} - \Delta \ln a \left[1 - H(\tilde{z}) \frac{\partial}{\partial \tilde{z}} \left(\frac{1 + \tilde{z}}{H(\tilde{z})} \right) \right] - A - v_{\parallel} + B_{\parallel}$$

$$+ \frac{1 + \tilde{z}}{H(\tilde{z})} \left(-\partial_{\parallel} A + \partial_{\parallel} v_{\parallel} + \dot{B}_{\parallel} - \dot{v}_{\parallel} + \frac{1}{2} \dot{h}_{\parallel} \right). \quad (52)$$

The first line contains the contributions due to the fact that the size of the ruler evolves in time, the scale factor at emission is perturbed from $1/(1 + \tilde{z})$, and the fact that the distance-redshift relation evolves, in addition to the perturbation to the metric at the source location ($-A$) and the projection from coordinate-time to proper-time hypersurfaces ($B_{\parallel} - v_{\parallel}$). The contributions from the line-of-sight derivative of the line-of-sight displacements ($\propto (1 + \tilde{z})/H(\tilde{z})$) are given in the second line. Note the term $\partial_{\parallel} v_{\parallel}$, which is the dominant term on small scales in the conformal-Newtonian gauge. This term is also responsible for the linear redshift-space distortions [28]. Apart from the perturbation to the scale factor at emission, \mathcal{C} does not involve any integral terms; this is expected since \mathcal{C} is the only term remaining if the two lines of sight coincide ($\hat{\mathbf{n}} = \hat{\mathbf{n}}'$). In this case, the two rays share the same path from the closer of the two emission points, and no quantities integrated along the line of sight can contribute to the perturbation of the ruler.

Restricting to the synchronous-comoving and conformal-Newtonian gauges, respectively, we obtain

$$(\mathcal{C})_{\text{sc}} = -(\Delta \ln a)_{\text{sc}} \left[1 - \frac{d \ln r_0(\tilde{a})}{d \ln \tilde{a}} - H(\tilde{z}) \frac{\partial}{\partial \tilde{z}} \left(\frac{1 + \tilde{z}}{H(\tilde{z})} \right) \right] + \frac{1 + \tilde{z}}{2H(\tilde{z})} \dot{h}_{\parallel}. \quad (53)$$

$$(\mathcal{C})_{\text{cN}} = \frac{d \ln r_0(\tilde{a})}{d \ln \tilde{a}} \mathcal{T}_{\text{cN}} - (\Delta \ln a)_{\text{cN}} \left[1 - H(\tilde{z}) \frac{\partial}{\partial \tilde{z}} \left(\frac{1 + \tilde{z}}{H(\tilde{z})} \right) \right] - \Psi - v_{\parallel} + \frac{1 + \tilde{z}}{H(\tilde{z})} \left(-\partial_{\parallel} \Psi + \partial_{\parallel} v_{\parallel} - \dot{v}_{\parallel} + \dot{\Phi} \right). \quad (54)$$

Note that in case of the sc-gauge expression, the redshift-space distortion term is included in the last term, through $\dot{h}_{\parallel}/2 = \dot{D} + \partial_{\parallel}^2 \dot{E}$. Fig. 3 shows the angular power spectrum of \mathcal{C} due to standard adiabatic scalar perturbations in a Λ CDM cosmology (the details of the calculation are given in Appendix F of [14]). Clearly, \mathcal{C} is of the same order as the matter density contrast in synchronous-comoving gauge on all scales. In particular, the velocity gradient term dominates over all other contributions.

4.4. Vector

Next, we have the two-component vector, which can be written as

$$\mathcal{B}_i = -v_{\perp i} + B_{\perp i} + \frac{1 + \tilde{z}}{H(\tilde{z})} \partial_{\perp i} \Delta \ln a. \quad (55)$$

As expected, this vector involves the transverse derivative of the line-of-sight displacement and the line-of-sight derivative of the transverse displacement. Note that these two quantities are *not* observable individually.

Using the spin ± 1 unit vectors \mathbf{m}_{\pm} , \mathcal{B}_i can be decomposed into spin ± 1 components:

$$\begin{aligned} \mathcal{B}_i &= {}_{+1}\mathcal{B} m_+^i + {}_{-1}\mathcal{B} m_-^i \\ {}_{\pm 1}\mathcal{B} &\equiv m_{\mp}^i \mathcal{B}_i = -v_{\pm} + B_{\pm} + \frac{1 + \tilde{z}}{H(\tilde{z})} \partial_{\pm} \Delta \ln a, \end{aligned} \quad (56)$$

where we have used the notation of Equation (9). Similar to before, we can specialize this general result to the synchronous-comoving and conformal-Newtonian gauges:

$$({}_{\pm 1}\mathcal{B})_{\text{sc}} = \frac{1 + \tilde{z}}{2H(\tilde{z})} \int_0^{\tilde{x}} d\chi \frac{\chi}{\tilde{\chi}} \partial_{\pm} \dot{h}_{\parallel} \quad (57)$$

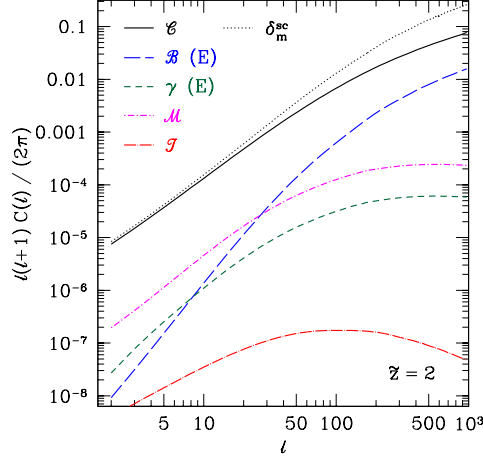


Figure 3. Angular power spectra of the different standard ruler perturbations produced by a standard scale-invariant power spectrum of curvature perturbations: \mathcal{C} , E -mode of \mathcal{B}_i , E -mode of the shear γ , magnification \mathcal{M} , and clock perturbation \mathcal{T} . \mathcal{C} and \mathcal{M} are calculated for a non-evolving ruler, and all are for a sharp source redshift of $\bar{z} = 2$. For comparison, the thin dotted line shows the angular power spectrum at $z = 2$ of the matter density field in synchronous-comoving gauge. Note that all quantities shown here, except for δ_m^{sc} , are gauge-invariant and (in principle) observable. Adapted from [14, 16].

$$\begin{aligned}
 (\pm 1 \mathcal{B})_{\text{cN}} &= -v_{\pm} + \frac{1 + \bar{z}}{H(\bar{z})} \partial_{\pm} \Delta \ln a \\
 &= -v_{\pm} + \frac{1 + \bar{z}}{H(\bar{z})} \left(-\partial_{\pm} \Psi + \partial_{\pm} [v_{\parallel} - v_{\parallel o}] + \int_0^{\bar{x}} d\chi \frac{\chi}{\bar{\chi}} \partial_{\pm} (\dot{\Phi} - \dot{\Psi}) \right). \quad (58)
 \end{aligned}$$

On small scales, the dominant contribution to \mathcal{B}_i comes from the transverse derivative of the line-of-sight component of the velocity $\partial_{\pm} v_{\parallel}$, which is of the same order as the tidal field.

Applying the spin-lowering operator $\bar{\partial}$ to ${}_1\mathcal{B}$ yields a spin-zero quantity (see Appendix A of [14]), which can be expanded in terms of the usual spherical harmonics. We then obtain the multipole coefficients of \mathcal{B} as

$$a_{lm}^{\mathcal{B}}(\bar{z}) = -\sqrt{\frac{(l-1)!}{(l+1)!}} \int d\Omega [\bar{\partial} {}_1\mathcal{B}(\hat{\mathbf{n}}, \bar{z})] Y_{lm}^*(\hat{\mathbf{n}}). \quad (59)$$

An equivalent result is obtained for $\bar{\partial} {}_{-1}\mathcal{B}$. In general, the multipole coefficients $a_{lm}^{\mathcal{B}}$ are complex, so that we can decompose them into real and imaginary parts,

$$a_{lm}^{\mathcal{B}} = a_{lm}^{\mathcal{B}E} + i a_{lm}^{\mathcal{B}B}. \quad (60)$$

One can easily show (Appendix A of [14]) that under a change of parity $a_{lm}^{\mathcal{B}E}$ transform as the spherical harmonic coefficients of a vector (parity-odd), whereas $a_{lm}^{\mathcal{B}B}$, picking up an additional minus sign, transform as those of a pseudo-vector (parity-even). These thus correspond to the polar (“ E ”) and axial (“ B ”) parts of the vector \mathcal{B}_i . As required by parity, scalar perturbations do not contribute to the axial part $a_{lm}^{\mathcal{B}B}$. Thus, a measurement of the vector component \mathcal{B}_i of standard ruler distortions offers an additional possibility to probe gravitational waves with large-scale structure, as

tensor modes do contribute to $a_{lm}^{\mathcal{B}\mathcal{B}}$. Thus, in principle the axial component of \mathcal{B}_i could be of similar interest for constraining tensor modes as weak lensing B -modes [15].

The power spectrum of the E -mode of \mathcal{B} due to standard scalar perturbations is shown in Figure 3. The dominant contribution to \mathcal{B}_i for a given Fourier mode of the matter density contrast in synchronous-comoving gauge is $\propto k_\perp k_\parallel / k^2 \delta_m^{\text{sc}}(\mathbf{k}, \tilde{z})$, while the corresponding contribution to the longitudinal scalar \mathcal{C} is $\propto k_\parallel^2 / k^2 \delta_m^{\text{sc}}(\mathbf{k}, \tilde{z})$. Even though approximate scaling arguments suggest that $C_{\mathcal{C}}(l)$, $C_{\mathcal{B}}^{EE}(l)$ should scale roughly equally with l , the different structure in terms of k_\parallel , k_\perp (together with the shape of the matter power spectrum in Λ CDM) leads to a faster scaling of $C_{\mathcal{B}}(l)$ with l for $l \lesssim 500$ (see discussion in [14]).

4.5. Transverse tensor: shear and magnification

Finally, we have the purely transverse component,

$$\mathcal{A}_{ij} = \frac{d \ln r_0(\tilde{a})}{d \ln \tilde{a}} \mathcal{T} \mathcal{P}_{ij} - \Delta \ln a \mathcal{P}_{ij} - \frac{1}{2} \mathcal{P}_i^k \mathcal{P}_j^l h_{kl} - \partial_\perp ({}_i \Delta x_{\perp j}) - \frac{1}{\tilde{\chi}} \Delta x_{\parallel} \mathcal{P}_{ij}, \quad (61)$$

where we have again inserted projection operators for clarity (note that \mathcal{P}_{ij} serves as the identity matrix on the sphere). As a symmetric matrix on the sphere, \mathcal{A}_{ij} has a scalar component, given by the trace \mathcal{A} , and two components of the traceless part which transform as spin-2 fields on the sphere. The trace corresponds to the change in area on the sky subtended by two perpendicular standard rulers. Thus, it is equal to the magnification \mathcal{M} (see also Fig. 2). The two components of the traceless part correspond to the shear γ . If we choose a fixed coordinate system $(\mathbf{e}_\theta, \mathbf{e}_\phi, \hat{\mathbf{n}})$, we can thus write

$$\mathcal{A}_{ij} = \begin{pmatrix} \mathcal{M}/2 + \gamma_1 & \gamma_2 \\ \gamma_2 & \mathcal{M}/2 - \gamma_1 \end{pmatrix}. \quad (62)$$

Below, we will derive the magnification and shear for the general perturbed FRW metric Equation (1).

4.5.1. Magnification

Taking the trace of Equation (61) yields

$$\mathcal{M} \equiv \mathcal{P}^{ij} \mathcal{A}_{ij} = 2 \frac{d \ln r_0(\tilde{a})}{d \ln \tilde{a}} \mathcal{T} - 2 \Delta \ln a - \frac{1}{2} (h - h_\parallel) - \frac{2}{\tilde{\chi}} \Delta x_{\parallel} + 2\hat{\kappa}. \quad (63)$$

The magnification is directly related to the fractional perturbation in the angular diameter and luminosity distances (see [29, 30]) through

$$\frac{\Delta D_L}{D_L} = \frac{\Delta D_A}{D_A} = -\frac{1}{2} \mathcal{M}, \quad (64)$$

where the first equality for the luminosity distance follows from the conservation of the photon phase space density. That is, \mathcal{M} describes both the change in apparent angular size of a spatial ruler as well as the change in observed flux of a standard candle. The contributions to the magnification are straightforwardly interpreted as coming from the time evolution of ruler scale (or intrinsic source luminosity, if applied to standard candles) through the proper time perturbation \mathcal{T} ; from the conversion of coordinate distance to physical scale at the source (both from the perturbation to the scale factor $\Delta \ln a$ and the metric at the source projected perpendicular to the line of

sight, $h - h_{\parallel}$); from the fact that the entire ruler is moved closer or further away by Δx_{\parallel} ; and finally from the coordinate convergence $\hat{\kappa}$ defined through

$$\hat{\kappa} = -\frac{1}{2}\partial_{\perp i}\Delta x_{\perp}^i. \quad (65)$$

This term is the dominant contribution to \mathcal{M} on small scales. However, the coordinate convergence is a gauge-dependent quantity; see for example Appendix B2 in [11]. In conformal-Newtonian gauge, it assumes its familiar form,

$$(\hat{\kappa})_{\text{cN}} = -v_{\parallel o} + \frac{1}{2}\int_0^{\tilde{\chi}} d\chi \frac{\chi}{\tilde{\chi}}(\tilde{\chi} - \chi)\nabla_{\perp}^2(\Psi - \Phi), \quad (66)$$

with an additional term $-v_{\parallel o}$ contributing to the dipole of $\hat{\kappa}$ only, which corresponds to the relativistic aberration effect at linear order. An explicit expression for the magnification in general gauge is straightforward to obtain, however it becomes lengthy. Here we just give the results for the two most popular gauge choices. First, in synchronous-comoving gauge [Equation (2)] we obtain

$$(\mathcal{M})_{\text{sc}} = 2\left[\frac{d\ln r_0(\tilde{a})}{d\ln \tilde{a}} - 1\right](\Delta \ln a)_{\text{sc}} - \frac{1}{2}(h - h_{\parallel}) + 2(\hat{\kappa})_{\text{sc}} - \frac{2}{\tilde{\chi}}\Delta x_{\parallel}, \quad (67)$$

where

$$(\hat{\kappa})_{\text{sc}} = -\frac{1}{4}[h_o - 3(h_{\parallel})_o] + \frac{1}{2}\int_0^{\tilde{\chi}} d\chi \left[(\partial_{\perp}^l h_{lk})\hat{n}^k + \frac{1}{\chi}(h - 3h_{\parallel}) - \frac{1}{2}(\tilde{\chi} - \chi)\frac{\chi}{\tilde{\chi}}\nabla_{\perp}^2 h_{\parallel} \right].$$

In conformal-Newtonian gauge [Equation (3)], we have $(h - h_{\parallel})/2 = 2\Phi$, so that the magnification in this gauge becomes

$$\begin{aligned} (\mathcal{M})_{\text{cN}} &= 2\frac{d\ln r_0(\tilde{a})}{d\ln \tilde{a}}\mathcal{T}_{\text{cN}} + \left[-2 + \frac{2}{aH\tilde{\chi}}\right](\Delta \ln a)_{\text{cN}} - 2\Phi + 2(\hat{\kappa})_{\text{cN}} \\ &\quad - \frac{2}{\tilde{\chi}}\int_0^{\tilde{\chi}} d\chi(\Psi - \Phi) + \frac{2}{\tilde{\chi}}\int_0^{t_o} dt\Psi(\mathbf{0}, t). \end{aligned} \quad (68)$$

The last term in Equation (68) is a pure monopole and thus usually absorbed in the ruler calibration (since r_0 can rarely be predicted from first principles without any dependence on the background cosmology). Nevertheless, the monopole of \mathcal{M} is in principle observable, and including this term ensures that gauge modes (for example superhorizon metric perturbations) do not affect its value.

We have thus arrived at a general gauge-invariant expression for the magnification without having to perform lengthy calculations. Moreover, the physical starting point from a standard ruler scale has allowed us to identify a previously overlooked contribution to the magnification. This contribution is given by the clock variable \mathcal{T} and becomes relevant whenever the ruler scale evolves over cosmic time. In many applications, this is the case, although \mathcal{T} is sub-dominant to the lensing convergence $\hat{\kappa}$ on all but the largest scales [16].

4.5.2. Shear We now consider the traceless part of \mathcal{A}_{ij} , given by

$$\begin{aligned} \gamma_{ij}(\hat{\mathbf{n}}) &\equiv \mathcal{A}_{ij} - \frac{1}{2}\mathcal{P}_{ij}\mathcal{M} \\ &= -\frac{1}{2}\left(\mathcal{P}_i^k\mathcal{P}_j^l - \frac{1}{2}\mathcal{P}_{ij}\mathcal{P}^{kl}\right)h_{kl} - \partial_{\perp(i}\Delta x_{\perp j)} - \mathcal{P}_{ij}\hat{\kappa}. \end{aligned} \quad (69)$$

Here, the terms $\propto \mathcal{P}_{ij}$ in Equation (61) drop out. The last two terms here are what commonly is regarded as the shear, i.e. the trace-free part of the transverse derivatives of the transverse displacements. The first term on the other hand is important to construct an *observable* as it ensures a gauge-invariant result. This is the term referred to as “metric shear” in [13]. Its physical significance becomes clear when constructing the Fermi normal coordinates, or local inertial frame, for the region containing the standard ruler.

Consider a region of spatial extent R , say centered on a given galaxy, and enclosing our standard ruler. We can construct orthonormal Fermi normal coordinates [31, 32] around the center of this region, which follows a timelike geodesic, by choosing the origin to be located at the center of the region at all times, and the time coordinate to be the proper time along the geodesic. As a local inertial frame, the spacetime in the Fermi coordinates (t_F, x_F^i) is Minkowski close to the geodesic, with corrections proportional to \mathbf{x}_F^2/R_c^2 where R_c is the curvature scale of the spacetime. Thus, as long as these corrections to the metric are negligible, there is no preferred direction in this frame, and the size r_0 of the standard ruler has to be (statistically) independent of the orientation. The most obvious example is galaxy shapes, which are used for cosmic shear measurements. In the Fermi frame, when neglecting tidal alignments, galaxy orientations are statistically random. As shown in [14, 15], the transformation from global coordinates to Fermi coordinates for a purely spatial metric perturbation h_{ij} is given by

$$a^{-1}x_F^i = x^i + \frac{1}{2}h_{ij}(0)x^j + \mathcal{O}(\partial_m h_{kl}x^2). \quad (70)$$

In order to obtain the shear relative to the Fermi frame, we need to add the transformation Equation (70) to the displacements Δx^i :

$$\Delta x^i \rightarrow \Delta x^i + \frac{1}{2}h_{ij}(0)x^j. \quad (71)$$

With these new displacements, the transverse derivative of the transverse displacement becomes

$$\partial_{\perp(i}\Delta x_{\perp j)} \rightarrow \partial_{\perp(i}\Delta x_{\perp j)} + \frac{1}{2}\mathcal{P}_i^k\mathcal{P}_j^l h_{kl} + \mathcal{O}(\partial_k h_{ij}[\tilde{\mathbf{x}} - \tilde{\mathbf{x}}']), \quad (72)$$

where the last term is negligible in the small-ruler approximation. This agrees exactly with the result derived above, Equation (69) [after subtracting the trace of Equation (72)]. Note that the Fermi coordinates are uniquely determined up to three Euler angles. The statement that galaxy orientations are random in this frame is thus coordinate-invariant.

γ_{ij} is a symmetric trace-free tensor on the sphere, and can thus be decomposed into spin ± 2 components (in analogy to the polarization of the CMB). Following Appendix A in [14] (see also [33]) we can write γ_{ij} as

$$\begin{aligned} \gamma_{ij} &= 2\gamma m_+^i m_+^j + -2\gamma m_-^i m_-^j \\ \pm 2\gamma &= m_{\mp}^i m_{\mp}^j \gamma_{ij}, \end{aligned} \quad (73)$$

where $\pm 2\gamma$ are spin ± 2 functions on the sphere (in analogy to the combination of Stokes parameters $Q \pm iU$). The general, lengthy expression for the shear components can be found in [14]. Here we give the expressions for the synchronous-comoving (sc) and the conformal-Newtonian (cN) gauges (note that $h_{\pm} = 0$ in cN gauge):

$$(\pm 2\gamma)_{\text{sc}} = -\frac{1}{2}h_{\pm} - \frac{1}{2}(h_{\pm})_o - \int_0^{\tilde{\chi}} d\chi \left[\left(1 - 2\frac{\chi}{\tilde{\chi}}\right) (\partial_{\pm} h_{kl}) m_{\mp}^k \hat{n}^l - \frac{1}{\tilde{\chi}} h_{\pm} \right] \quad (74)$$

$$\begin{aligned}
 & + (\tilde{\chi} - \chi) \frac{\chi}{\tilde{\chi}} \frac{1}{2} (m_{\mp}^i m_{\mp}^j \partial_i \partial_j h_{lk}) \hat{n}^l \hat{n}^k \Big] \\
 (\pm 2\gamma)_{cN} = & \int_0^{\tilde{\chi}} d\chi (\tilde{\chi} - \chi) \frac{\chi}{\tilde{\chi}} m_{\mp}^i m_{\mp}^j \partial_i \partial_j (\Psi - \Phi). \quad (75)
 \end{aligned}$$

We see that Equation (75) recovers the “standard” result; in other words, there are no additional relativistic corrections to the shear *in cN gauge*. This is not surprising following our arguments above: in the conformal-Newtonian gauge, the transformation Equation (70) from global coordinates to the local Fermi frame is isotropic since $h_{ij} = 2\Phi\delta_{ij}$. Thus, it does not contribute to the shear. Note however that this only applies to scalar perturbations; when considering vector or tensor perturbations, Equation (74) is the relevant expression which does contain terms beyond the derivative of the deflection angle. This is also of relevance to studies of gravitational lensing of the CMB by gravitational waves [34] (see also [15]).

Fig. 3 shows the angular power spectrum of shear and magnification due to scalar perturbations for a sharp source redshift $\tilde{z} = 2$. For $l \gtrsim 10$, the results follow the familiar relation $C_{\mathcal{M}}(l) = 4C_{\gamma}^{EE}(l)$, valid when all relativistic corrections to the magnification become irrelevant so that $\mathcal{M} \simeq 2\hat{\kappa}$. These corrections slightly increase the magnification for small l . We also see that γ and \mathcal{M} are suppressed with respect to \mathcal{C} and \mathcal{B} (on smaller scales), at least when the latter are evaluated for a sharp source redshift. This is a well-known consequence of the projection with the broad lensing kernel, leading to a cancellation of modes that are not purely transverse (see e.g. [35]).

4.6. Applications

Consider a galaxy whose image projected on the sky, as seen by a local observer, has an “intrinsic” intensity or surface brightness $I(\boldsymbol{\theta})$ (here $\boldsymbol{\theta} = 0$ corresponds to the centroid of the galaxy). Then, the ruler formalism immediately yields the observed intensity through

$$I_{\text{obs}}(\tilde{\boldsymbol{\theta}}^i) = I\left(\tilde{\boldsymbol{\theta}}^i - \mathcal{A}_i^j \tilde{\boldsymbol{\theta}}^j\right) = \left[1 - \mathcal{A}_i^j \tilde{\boldsymbol{\theta}}^i \frac{\partial}{\partial \tilde{\boldsymbol{\theta}}^j}\right] I(\tilde{\boldsymbol{\theta}}) + \mathcal{O}([\mathcal{A}_{ij}]^2), \quad (76)$$

where \mathcal{A}_{ij} is the sky-plane projection of the ruler perturbations, Equation (51), and we have expanded to linear order. This is the well known effect of weak gravitational lensing on an image.

Now consider the case of a spectroscopic survey, where we measure the small-scale correlation function $\tilde{\xi}(\tilde{\mathbf{r}}, \tilde{z})$ as a function of the three-dimensional separation vector $\tilde{\mathbf{r}}$ and the redshift \tilde{z} . As shown in [36], the observed correlation function is given in terms of the expectation value of the intrinsic correlation function $\xi(r, z)$ by

$$\tilde{\xi}(\tilde{\mathbf{r}}, \tilde{\tau}) = \left[1 - a_{ij}(\tilde{x}) \tilde{\mathbf{r}}^i \partial_{\tilde{r}}^j + \mathcal{T}(\tilde{x}) \partial_{\tilde{z}} + 2\langle\tilde{\delta}\rangle(\tilde{x})\right] \xi(\tilde{\mathbf{r}}; \tilde{z}), \quad (77)$$

where $\langle\tilde{\delta}\rangle$ is the mean observed overdensity of the tracer within the volume over which $\tilde{\xi}$ is measured (see the next section), which simply serves to rescale the local mean density. The tensor a_{ij} contains the ruler perturbations:

$$a_{ij} = \mathcal{C} \hat{n}_i \hat{n}_j + \hat{n}_{(i} \mathcal{P}_{j)k} \mathcal{B}^k + \mathcal{P}_{ik} \mathcal{P}_{jl} \mathcal{A}^{kl}, \quad (78)$$

where we have inserted trivial projection operators for \mathcal{B} , \mathcal{A} .

These examples serve to illustrate how the standard ruler formalism can be immediately applied to predict cosmological observables.

5. Galaxy clustering

The statistics (correlation functions) of large-scale structure tracers have a long history as one of the most important observational tools in cosmology. The fundamental building block of these statistics is the observed number density \tilde{n}_g of tracers inferred from their apparent positions on the sky and redshifts. In this section, we show how \tilde{n}_g is related to the spacetime perturbations in the relativistic context. For this, we need to consider two effects: first, the effect of spacetime perturbations on the propagation of light emitted from the sources systematically distorts the observed galaxy density contrast [7, 8, 9, 10, 37, 11, 12]. Second, we need to relate the number density of galaxies to the matter density, a procedure commonly known as *biasing*, which involves additional subtleties in the relativistic context [37, 11].

As discussed earlier in § 2.2, observers chart galaxies according to the observed position $\tilde{x}^\mu = (\eta_0 - \tilde{\chi}, \hat{\mathbf{n}}\tilde{\chi})$. The galaxy density is estimated based on the observed spatial coordinate $\tilde{\mathbf{x}} = \tilde{\chi}\hat{\mathbf{n}}$, and then compared with the *mean* number density $\tilde{n}_g(\tilde{z})$ at fixed observed coordinate to infer the local galaxy overdensity $\tilde{\delta}_g$. Once corrected for window function and selection effects, the mean galaxy number density only depends on the observed redshift. In this sense, the observed density contrast $\tilde{\delta}_g$ can be seen as defined in a constant-observed-redshift gauge. Throughout, we will assume that $\tilde{n}_g(z)$ corresponds to the true mean density of galaxies, i.e. we will neglect the effect of super-survey modes.

The number of galaxies enclosed in a spatial volume V defined in the observed coordinates is given by

$$N(V) = \int_V d^3\tilde{\mathbf{x}} \sqrt{-g(x)} n_g(x) \varepsilon_{\mu\nu\rho\sigma} u^\mu(x) \frac{\partial x^\nu}{\partial \tilde{x}^1} \frac{\partial x^\rho}{\partial \tilde{x}^2} \frac{\partial x^\sigma}{\partial \tilde{x}^3}, \quad (79)$$

where we have transformed the integral to observed coordinates \tilde{x} , V is a spatial volume on a constant-observed-redshift slice, and $x(\tilde{x})$ denotes the true spacetime location corresponding to the observed location \tilde{x} . n_g is the physical (as opposed to comoving) number density of tracers in the perturbed FRW coordinates [Eq. (1)].

We now employ a useful trick. Rather than expressing n_g in terms of the galaxy density perturbation δ_g in some arbitrary gauge, we fix the coordinates to the *constant-observed-redshift* (“or”) *gauge*. We thus write n_g in term of the mean number density \tilde{n}_g and the perturbation δ_g^{or} to the comoving number density in the constant-observed-redshift gauge as

$$a^3 n_g(x) = \tilde{a}^3 \tilde{n}_g(\tilde{z}) [1 + \delta_g^{\text{or}}(\mathbf{x}, \tilde{z})], \quad (80)$$

where \tilde{z} is the observed redshift corresponding to the spacetime location x , and $\tilde{a} = 1/(1 + \tilde{z})$. Since δ_g^{or} is already first order, we can neglect the distinction between $\mathbf{x}(\tilde{x})$ and $\tilde{\mathbf{x}}$ in its argument. Eq. (80) can be understood as the definition of δ_g^{or} .

We rewrite the right hand side of Eq. (79) in terms of the metric perturbation to linear order as

$$N(V) = \int_V d^3\tilde{\mathbf{x}} \left(1 + A + \frac{h}{2}\right) \tilde{a}^3 \tilde{n}_g(\tilde{z}) [1 + \delta_g^{\text{or}}(\tilde{\mathbf{x}}, \tilde{z})] \left((1 - A) \left| \frac{\partial x^i}{\partial \tilde{x}^j} \right| + v_{\parallel} \right). \quad (81)$$

The observed galaxy number density \tilde{n}_g , on the other hand, satisfies by definition

$$N = \int d^3\tilde{\mathbf{x}} \tilde{a}^3 \tilde{n}_g(\tilde{\mathbf{x}}, \tilde{z}). \quad (82)$$

By equating the two, we find the observed galaxy density contrast as

$$\tilde{\delta}_g(\tilde{\mathbf{x}}) \equiv \frac{\tilde{n}_g(\tilde{\mathbf{x}}, \tilde{z})}{\tilde{n}_g(\tilde{z})} - 1 = \delta_g^{\text{or}}(\tilde{\mathbf{x}}, \tilde{z}) + \frac{h}{2} + \partial_{\parallel} \Delta x_{\parallel} + \frac{2\Delta x_{\parallel}}{\tilde{\chi}} - 2\hat{\kappa} + v_{\parallel}. \quad (83)$$

Here, we have used the Jacobian

$$\left| \frac{\partial x^i}{\partial \tilde{x}^j} \right| = 1 + \frac{\partial \Delta x^i}{\partial \tilde{x}^i} = 1 + \partial_{\parallel} \Delta x_{\parallel} + \frac{2\Delta x_{\parallel}}{\tilde{\chi}} - 2\hat{\kappa} \quad (84)$$

with the lensing convergence $\hat{\kappa}$ defined in Equation (65). All contributions in Eq. (83) apart from δ_g^{or} thus correspond to the apparent modulation of the galaxy abundance due to volume distortion effects.

Next, we have to relate δ_g^{or} in Equation (83) to the matter density through a biasing relation. The galaxy density contrast δ_g^{or} in Equation (83) is defined in the constant-observed-redshift slicing, while the linear bias relation between galaxy density contrast and matter density contrast holds only on *constant-proper-time* (“pt”) slices. This is because in the large-scale limit, galaxies only know about the local age of the Universe and the local matter density (see [37] and §III in [11] for a detailed discussion). ^{\mathcal{P}} The shift between the constant-observed-redshift slice and constant-proper-time slice is given by the observable \mathcal{T} that we have discussed in § 3. Then, the relation between $\delta_g^{\text{or}}(\tilde{\mathbf{x}}, \tilde{z})$ and the matter perturbation δ_m^{pt} in the constant-proper-time (or synchronous) gauge is given by the standard linear gauge transformation

$$\delta_g^{\text{or}}(\tilde{\mathbf{x}}, \tilde{z}) = b \delta_m^{\text{pt}} + \frac{d(a^3 \bar{n}_g)}{d \ln a} \mathcal{T} \equiv b \delta_m^{\text{pt}} + b_e \mathcal{T}, \quad (85)$$

where we have introduced the dimensionless parameter b_e quantifying the evolution of the mean comoving number density of tracers. Note that this relation only involves observable quantities, so that both b and b_e are well defined and gauge-invariant. It also serves as the unambiguous starting point for extending the bias relation to higher order in perturbations, for example by adding a term $b_2/2 (\delta_m^{\text{pt}})^2$ to the right hand side.

Finally, δ_m^{pt} is related to the matter density perturbation δ_m in the chosen gauge through

$$\delta_m^{\text{pt}} = \delta_m + 3\tilde{H} \int_0^{\tilde{\eta}} A(\mathbf{x}, \eta) a(\eta) d\eta. \quad (86)$$

Combining the last two equations, we find the galaxy density contrast on the constant-observed-redshift slice in terms of the density contrast in an arbitrary gauge as

$$\delta_g^{\text{or}}(\tilde{\mathbf{x}}, \tilde{z}) = b \left[\delta_m + 3\tilde{H} \int_0^{\tilde{\eta}} A(\mathbf{x}, \eta) a(\eta) d\eta \right] + b_e \mathcal{T}. \quad (87)$$

This yields our final expression:

$$\tilde{\delta}_g(\tilde{\mathbf{x}}, \tilde{z}) = b \left[\delta_m + 3\tilde{H} \int_0^{\tilde{\eta}} A(\mathbf{x}, \eta) a(\eta) d\eta \right] + b_e \mathcal{T} + \frac{1}{2}h + \partial_{\tilde{\chi}} \Delta x_{\parallel} + \frac{2\Delta x_{\parallel}}{\tilde{\chi}} - 2\hat{\kappa} + v_{\parallel}. \quad (88)$$

^{\mathcal{P}} This assumes that there are no additional degrees of freedom relevant on large scales, such as dark energy perturbations, neutrinos, or fifth forces. The impact of these on the general linear biasing relation is an interesting question, though beyond the scope of this review.

Here,

$$\begin{aligned} \partial_{\tilde{x}} \Delta x_{\parallel} = & A - B_{\parallel} - \frac{1}{2} h_{\parallel} - H(\tilde{z}) \frac{\partial}{\partial \tilde{z}} \left(\frac{1 + \tilde{z}}{H(\tilde{z})} \right) \Delta \ln a \\ & - \frac{1 + \tilde{z}}{H(\tilde{z})} \left(-\partial_{\parallel} A + \partial_{\parallel} v_{\parallel} - \dot{v}_{\parallel} + \frac{1}{2} \dot{h}_{\parallel} + \dot{B}_{\parallel} \right). \end{aligned} \quad (89)$$

One subtlety we have neglected so far is that observational selection effects can modify the observed galaxy density, Equation (88). Usually surveys observe galaxies above a certain magnitude threshold. Weak lensing magnifies/de-magnifies the flux of the source galaxies and therefore induces another contribution to the observed galaxy density (*magnification bias*). For a population of galaxies at fixed redshift \tilde{z} with cumulative luminosity function $\bar{n}(> L_{\min})$, we define

$$\mathcal{Q} \equiv - \frac{d \ln \bar{n}(> L_{\min})}{d \ln L_{\min}}, \quad (90)$$

where \mathcal{M} is the magnification discussed in detail in § 4.5.1. Then, the contribution to $\tilde{\delta}_g$ induced by the lensing magnification [Equation (63)] is $\mathcal{Q} \mathcal{M}$. Note that our “ruler” here is the luminosity of galaxies at the cutoff L_{\min} , so that $d \ln r_0 / d \ln a$ in Eq. (63) is to be replaced with the evolution of the intrinsic luminosity of galaxies with $L = L_{\min}$ at \tilde{z} , $d \ln L_{\min} / d \ln a$, in order to take the evolving ruler effect into account (§ 4.1). We finally obtain the observed density contrast including magnification bias as

$$\begin{aligned} \tilde{\delta}_g(\tilde{\mathbf{x}}, \tilde{z}) = & b \left[\delta_m + 3\tilde{H} \int_0^{\tilde{\eta}} A(\mathbf{x}, \eta) a(\eta) d\eta \right] + \left(b_e + 2\mathcal{Q} \left[\frac{d \ln L_{\min}}{d \ln a} - 1 \right] \right) \mathcal{T} \\ & + 2\mathcal{Q}\tilde{H} \int_0^{\tilde{\eta}} A(\mathbf{x}, \eta) a(\eta) d\eta + \frac{1}{2} (1 - \mathcal{Q}) h + \frac{\mathcal{Q}}{2} h_{\parallel} + \partial_{\tilde{x}} \Delta x_{\parallel} + (1 - \mathcal{Q}) \frac{2}{\tilde{\chi}} \Delta x_{\parallel} \\ & - 2(1 - \mathcal{Q}) \hat{\kappa} + v_{\parallel}. \end{aligned} \quad (91)$$

Eq. (91) provides the complete result for the observed overdensity of a tracer at linear order in a general gauge; to our knowledge, this is the first time an expression for $\tilde{\delta}_g$ has been given in a general gauge with a physical treatment of galaxy bias. When restricted to conformal-Newtonian gauge, this agrees with [10, 37] (note the discussion around Eq. (31) of the former reference); restricting to synchronous-comoving gauge yields the results derived in [11]. Note also that all previous references implicitly assumed that $d \ln L_{\min} / d \ln a$, which induces an apparent density contrast due to time evolution of the luminosity function, is zero (though since this term is proportional to \mathcal{T} , it is expected to be subdominant on all scales, see Fig. 3). Throughout, we have assumed a sharp source redshift. The projection over a wider photometric redshift bin is straightforward.

Assuming the coefficients b , b_e , \mathcal{Q} are all of order unity, the various terms in Eq. (91) can be ranked in terms of relative importance according to their scaling in Fourier space. The largest terms, “order 1”, are

$$\tilde{\delta}_g^{\mathcal{O}(1)} = b \delta_m + \frac{1 + \tilde{z}}{\tilde{H}} \partial_{\parallel} v_{\parallel} - 2(1 - \mathcal{Q}) \hat{\kappa}. \quad (92)$$

Here, we have assumed that one of the standard gauges is chosen where $\delta_m \simeq \delta_m^{\text{pt}}$ on small scales (this includes conformal-Newtonian gauge). Equation (92) is the standard small-scale result for the apparent galaxy overdensity, including the leading redshift-space distortion (“Kaiser formula” [28]) and magnification bias. Next, there are contributions suppressed by $\tilde{a}\tilde{H}/k$ (“velocity-type”) and $(\tilde{a}\tilde{H}/k)^2$ (“potential-type”).

The potential-type contributions have the same k -dependence as the scale-dependent bias from primordial non-Gaussianity of the local type [38]. These are numerically the smallest contributions, and amount to the effect of local primordial non-Gaussianity with $f_{\text{NL}} \lesssim 1$, as shown in [11]. The velocity-type contributions, which are $\propto v_{\parallel}$ and $\partial_{\parallel}\Psi$ in case of conformal-Newtonian gauge, are larger and likely to be measurable in upcoming surveys [39].

6. Conclusion and future work

In this paper, we have derived the effects of light deflection in the perturbed FRW universe, and an associated set of observables in the large-scale structure of the Universe. Light deflection distorts the observed position and redshift of cosmic events, and such distortions can be measured for events with known cosmic age (cosmic clock) or length scale (cosmic ruler). Distortions in the cosmic clocks are described by the observable \mathcal{T} , which is the redshift perturbation between the constant-proper-time slicing and the constant-observed-redshift slicing (an example being the CMB temperature perturbations in the Sachs-Wolfe limit); distortions in the cosmic rulers are completely described by six observables which are classified as two scalars (\mathcal{C} and the magnification \mathcal{M}), two components of a divergence-free vector (\mathcal{B}_i), and two components of a tensor (shear γ_{ij}) on the celestial sphere.

We have also presented the fully general expression for the observed galaxy density contrast at linear order, a fundamental galaxy clustering observable, including the volume distortion due to the light deflection, evolving number density, galaxy density bias, as well as the magnification bias generalized to evolving luminosity function.

All expressions in this paper are derived at linear order in density, velocity, and metric perturbations, but in their most general form, sometimes referred to as *gauge ready* form. Therefore, all expressions in this paper can be trivially restricted to any specific gauge. We show gauge-fixed examples for the conformal Newtonian (cN) gauge and synchronous comoving (sc) gauge in § 4. Extending the calculations to higher order should also be straightforward, albeit tedious, by following the logical steps described in this paper. In fact, three pre-prints ([40, 41, 42]) extending the calculation of the observed galaxy density contrast to second order have appeared by the time this paper was written.

In summary, we now have a general relativistic description for the complete set of large-scale observables of the large-scale structure (\mathcal{T} , \mathcal{C} , \mathcal{B}_i , \mathcal{M} , γ_{ij} as well as $\tilde{\delta}_g$). Hence, future work can focus on the applications of these results. In particular, in conjunction with future large-scale structure surveys mapping a significant fraction of the observable universe ($V \gtrsim 100 [\text{Gpc}/h]^3$) such as Euclid, LSST and SKA, we envisage three directions that this line of research should pursue:

First of all, all expressions shown in this paper, with the exception of the biasing relation, Eq. (85), only depend on kinematics of light propagation, and, therefore, hold for *any* metric theory of gravity. Non-smooth Dark Energy as well as modified gravity theories predict different relations between the aforementioned observables and the cosmic density perturbations than the standard Λ CDM or smooth Dark Energy scenarios. This effect has only recently been explored for galaxy clustering [43], and it would be interesting to see how large the impact could be in other large-scale structure observables.

The relativistic effects discussed here appear on near horizon scales $k \sim 0.001 h/\text{Mpc}$. Our expressions for \mathcal{T} , \mathcal{C} , \mathcal{B} , \mathcal{M} , γ , $\tilde{\delta}_g$ are valid on the full sky and

can immediately be used to calculate angular auto- and cross-correlations $C(\ell)$ on arbitrarily large scales. However, for spectroscopic surveys, angular correlations in many narrow redshift bins might not be the optimal approach. While on sufficiently small scales the flat-sky approximation can be used, on large scales conventional Fourier-basis decompositions must be modified to include the effects from sky curvature as well as time evolution of the cosmic structure [44, 45, 46].

Finally, going beyond the power spectrum, it is interesting to investigate the impact of relativistic effects on higher order correlation functions. In general, this requires the calculation of the relativistic observables to higher order, e.g. second order for the bispectrum of cosmic shear and galaxy clustering. However, most of the signal-to-noise in the bispectrum on very large scales is in the squeezed limit, where one large-scale mode is correlated with two small-scale modes. In this limit, one can use a trick to circumvent the second order calculation [36]. The bispectrum in this limit is then entirely determined by the linear order ruler distortions of the small-scale correlation function that are described in § 4.6 (along with any primordial contribution due to local-type primordial non-Gaussianity).

In summary, the relativistic effects that we discuss here must be included whenever very large scale modes are measured, and are thus crucial in order to fully exploit the information in future large-scale structure surveys. Fortunately, they can be accurately predicted in terms of only a few tracer-dependent free parameters.

References

- [1] Bennett C L, Larson D, Weiland J L, Jarosik N, Hinshaw G, Odegard N, Smith K M, Hill R S, Gold B, Halpern M, Komatsu E, Nolte M R, Page L, Spergel D N, Wollack E, Dunkley J, Kogut A, Limon M, Meyer S S, Tucker G S and Wright E L 2013 *Astrophys. J. Supp.* **208** 20 (*Preprint* 1212.5225)
- [2] Komatsu E, Bennett C L, Barnes C, Bean R, Bennett C L, Doré O, Dunkley J, Gold B, Greason M R, Halpern M, Hill R S, Hinshaw G, Jarosik N, Kogut A, Komatsu E, Larson D, Limon M, Meyer S S, Nolte M R, Odegard N, Page L, Peiris H V, Smith K M, Spergel D N, Tucker G S, Verde L, Weiland J L, Wollack E and Wright E L 2014 *Progress of Theoretical and Experimental Physics* **2014** 06B102 (*Preprint* 1404.5415)
- [3] Ade P A R *et al.* 2013 *arXiv:1303.5062* (*Preprint* 1303.5062)
- [4] Planck Collaboration, Ade P A R, Aghanim N, Armitage-Caplan C, Arnaud M, Ashdown M, Atrio-Barandela F, Aumont J, Baccigalupi C, Banday A J and *et al* 2013 *ArXiv e-prints* (*Preprint* 1303.5076)
- [5] Cole S *et al.* (2dFGRS) 2005 *MNRAS* **362** 505–534 (*Preprint* astro-ph/0501174)
- [6] Eisenstein D J *et al.* (SDSS) 2005 *Astrophys. J.* **633** 560–574 (*Preprint* astro-ph/0501171)
- [7] Yoo J, Fitzpatrick A L and Zaldarriaga M 2009 *PRD* **80** 083514+ (*Preprint* 0907.0707)
- [8] Yoo J 2010 *PRD* **82** 083508+ (*Preprint* 1009.3021)
- [9] Bonvin C and Durrer R 2011 *ArXiv e-prints* (*Preprint* 1105.5280)
- [10] Challinor A and Lewis A 2011 *ArXiv e-prints* (*Preprint* 1105.5292)
- [11] Jeong D, Schmidt F and Hirata C M 2012 *PRD* **85** 023504 (*Preprint* 1107.5427)
- [12] Jeong D and Schmidt F 2012 *PRD* **86** 083512 (*Preprint* 1205.1512)
- [13] Dodelson S, Rozo E and Stebbins A 2003 *Physical Review Letters* **91** 021301+ (*Preprint* arXiv:astro-ph/0301177)
- [14] Schmidt F and Jeong D 2012 *PRD* **86** 083527 (*Preprint* 1204.3625)
- [15] Schmidt F and Jeong D 2012 *PRD* **86** 083513 (*Preprint* 1205.1514)
- [16] Jeong D and Schmidt F 2013 *ArXiv e-prints* (*Preprint* 1305.1299)
- [17] Pyne T and Birkinshaw M 1993 *Astrophys. J.* **415** 459 (*Preprint* arXiv:astro-ph/9303020)
- [18] Sachs R K and Wolfe A M 1967 *Astrophys. J.* **147** 73+
- [19] Catelan P, Kamionkowski M and Blandford R D 2001 *MNRAS* **320** L7–L13 (*Preprint* arXiv:astro-ph/0005470)
- [20] Hirata C M and Seljak U 2004 *PRD* **70** 063526 (*Preprint* arXiv:astro-ph/0406275)
- [21] Brown M L, Taylor A N, Hambly N C and Dye S 2002 *MNRAS* **333** 501–509 (*Preprint* arXiv:astro-ph/0009499)

- [22] Blazek J, McQuinn M and Seljak U 2011 *JCAP* **5** 10 (*Preprint* 1101.4017)
- [23] Joachimi B, Mandelbaum R, Abdalla F B and Bridle S L 2011 *Astron. Astrophys.* **527** A26 (*Preprint* 1008.3491)
- [24] Pen U L, Sheth R, Harnois-Deraps J, Chen X and Li Z 2012 *ArXiv e-prints* (*Preprint* 1202.5804)
- [25] Schmidt F, Pajer E and Zaldarriaga M 2014 *PRD* **89** 083507 (*Preprint* 1312.5616)
- [26] Sachs R 1961 *Royal Society of London Proceedings Series A* **264** 309–338
- [27] Gluscevic V, Kamionkowski M and Cooray A 2009 *PRD* **80** 023510 (*Preprint* 0905.1687)
- [28] Kaiser N 1987 *MNRAS* **227** 1–21
- [29] Hui L and Greene P B 2006 *PRD* **73** 123526 (*Preprint* arXiv:astro-ph/0512159)
- [30] Bonvin C, Durrer R and Gasparini M A 2006 *PRD* **73** 023523+ (*Preprint* arXiv:astro-ph/0511183)
- [31] Fermi E 1922 *Atti Acad. Naz. Lincei Rend. Cl. Sci. Fiz. Mat. Nat.* **31** 21
- [32] Manasse F K and Misner C W 1963 *Journal of Mathematical Physics* **4** 735–745
- [33] Hu W 2000 *PRD* **62** 043007 (*Preprint* arXiv:astro-ph/0001303)
- [34] Book L G, Kamionkowski M and Souradeep T 2011 *ArXiv e-prints* (*Preprint* 1109.2910)
- [35] Jeong D, Schmidt F and Sefusatti E 2011 *PRD* **83** 123005 (*Preprint* 1104.0926)
- [36] Pajer E, Schmidt F and Zaldarriaga M 2013 *PRD* **88** 083502 (*Preprint* 1305.0824)
- [37] Baldauf T, Seljak U, Senatore L and Zaldarriaga M 2011 *ArXiv e-prints* (*Preprint* 1106.5507)
- [38] Dalal N, Doré O, Huterer D and Shirokov A 2008 *PRD* **77** 123514+ (*Preprint* 0710.4560)
- [39] Yoo J, Hamaus N, Seljak U and Zaldarriaga M 2012 *PRD* **86** 063514 (*Preprint* 1206.5809)
- [40] Yoo J and Zaldarriaga M 2014 *ArXiv e-prints* (*Preprint* 1406.4140)
- [41] Bertacca D, Maartens R and Clarkson C 2014 *ArXiv e-prints* (*Preprint* 1405.4403)
- [42] Di Dio E, Durrer R, Marozzi G and Montanari F 2014 *ArXiv e-prints* (*Preprint* 1407.0376)
- [43] Lombriser L, Yoo J and Koyama K 2013 *PRD* **87** 104019 (*Preprint* 1301.3132)
- [44] Yoo J and Desjacques V 2013 *PRD* **88** 023502 (*Preprint* 1301.4501)
- [45] Di Dio E, Montanari F, Lesgourgues J and Durrer R 2013 *JCAP* **11** 044 (*Preprint* 1307.1459)
- [46] Di Dio E, Montanari F, Durrer R and Lesgourgues J 2014 *JCAP* **1** 042 (*Preprint* 1308.6186)